JOURNAL OF MATERIALS SCIENCE 12 (1977) 1349–1354

Transmission electron microscopic study of defect structure in natural chalcopyrite ($CuFeS_2$)

L. E. MURR, SUZANNE L. LERNER
Department of Metallurgical and Materials Engineering, New Mexico Institute of Mining and Technology, Socorro, New Mexico, USA

Natural chalcopyrite ($CuFeS_2$) specimens from Golden, New Mexico and Transvaal, South Africa were examined by transmission electron microscopy. The defect structure was composed of dislocations, dislocation loops, tangles, and substructure (including dislocation networks), stacking faults on {1 1 2} (both intrinsic and extrinsic), and mechanical twins and twin-faults. Optical microscopy indicated a large grain structure (0.3 to 0.5 cm grain size) containing numerous large twins similar in size to the average grain diameter. It is concluded that the absence of superdislocations of the type 1/4 ⟨2 0 1⟩ is a result of the $CuFeS_2$ structure approximating more closely the sphalerite lattice as a result of the *c/a* ratio approaching 2. It is also concluded that the apparently low stacking fault free energy in $CuFeS_2$ will give rise to abundant mechanical twins accommodating large deformations, and this may be an important factor in the grinding and leaching of chalcopyrite concentrates. The observations suggest that the defect structure, particularly the occurrence of superdislocations and antiphase boundaries, might increase with a decrease in the *c/a* ratio for chalcopyrite structures, and this may have an important influence on the electrical and mechanical properties of compounds having the chalcopyrite structure.

1. Introduction

Compounds of the type $A^IB^{IV}C_2^V$ and $A^IB^{III}C_2^{VI}$, ternary chalcopyrite semiconductors, have received considerable attention recently as a result of the demonstrated and potential applications of such materials in nonlinear optics, luminescence, and related semiconductor devices [1–4]. Although the preparation, physical properties, and bond structure of such compounds has received the most of this attention, there seems to have been little effort devoted to the study of defect structures in such materials. Pasemann and Kilmanek [5] have presented a survey of possible lattice defects in the chalcopyrite structure specific to $ZnSiP_2$, while Pasemann *et al.* [6] have more recently demonstrated the existence of superdislocations in $ZnSiP_2$; these indicate that the chalcopyrite structure can be treated as a superlattice of the sphalerite structure.

Lattice defects in natural chalcopyrite ($CuFeS_2$) have been considered by Gerlach *et al.* [7] in connection with their possible role in determining the reaction rate during the leaching of chalcopyrite concentrates. Although experimental evidence strongly suggests that crystal defects can contribute significantly to the leaching rate of natural chalcopyrite [7–9], there has been no direct evidence for their presence, nor is there any indication of their possible character. It is not known, for example, whether the distortional line broadening of X-ray spectra [7], is the result of the increase in numbers of dislocations, stacking faults, or twins (which could produce an effective grain refinement), which have been shown to be possible in chalcopyrite-type lattices such as $ZnSiAs_2$, $ZnSnAs_2$ and $CdSnAs_2$ in the recent work of Monfort *et al.* [10].

The tetragonal chalcopyrite structure is derived from the cubic sphalerite (zinc blende) structure by the tetragonal compression which occurs as a result of the ordering of the atoms in the cation sub-lattice. The unit cell of chalcopyrite is doubled in comparison with that of sphalerite. As a result of this polymeric isomorphism, a wide range of crystal defects can be postulated as indicated above and in the references cited previously [5, 10]. Twins, particularly annealing twins, have been commonly observed on {1 1 2} planes in tetragonal metals for example [11].

The present investigation was undertaken because the chalcopyrite structure forms the basis of a number of ternary semiconductors of importance, because $CuFeS_2$ is intrinsically important as a major natural mineral source of copper, and because there has never been an attempt to investigate defect structures in natural $CuFeS_2$ by direct observations as has occurred for other mineral systems [12].

2. Experimental method

Two large pure natural chalcopyrite samples were obtained for the present study. One sample, from the San Pedro Mine of the Goldfilled Consolidated Mining Co., Golden, New Mexico, measured approximately 10 cm × 5 cm × 5 cm. A second sample from Transvaal, South Africa was slightly smaller. Each contained small quartz inclusions (grains) but these were not abundant and were segregated to areas along the chalcopyrite grain boundaries. Each chalcopyrite sample was cut into numerous 3 mm thick slices using a diamond saw and several slices were metallographically (mechanically) polished (using a 0.6 μm grit size) in order to allow phase-contrast observations for grain size determinations in a Vickers metallograph.

Polished samples were also examined by the Laue back-reflection technique using a G.E. XRD-5 X-ray unit in order to investigate the grain size, grain orientations, and the incidence of twinned grains. An attempt was made to produce electron-transparent thin sections by ion etching, but was unsuccessful because the ion damage and associated heating of the thinning area caused the chalcopyrite to crack and flake off.

Electron-transparent sections of the chalcopyrite samples were prepared by crushing the 3 mm slices and other random chunks. Small chips, approximately 1 mm on a side were placed between two 200 mesh electron microscope screen grids using a vacuum tweezer. The small fragments were chosen randomly after inspection to ensure relatively flat chips. They were observed in a Hitachi Perkin–Elmer H.U. 200F transmission electron microscope operated at 200 kV and employing a goniometer-tilt stage.

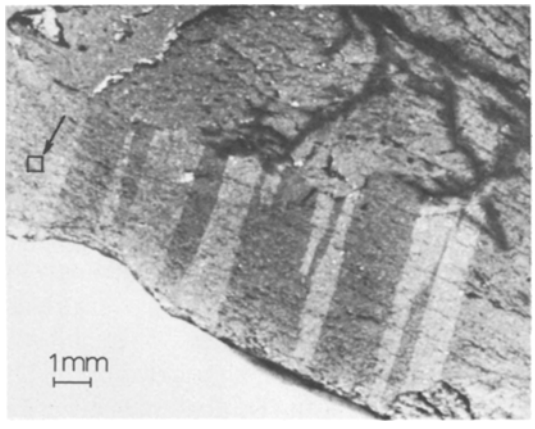

Figure 1 Chalcopyrite grain structure: small section of polished Golden, New Mexico, $CuFeS_2$ sample.

3. Results

Fig. 1 illustrates the chalcopyrite grain structure, and indicates that twinning is a prominent feature of the natural chalcopyrites examined. Twinning was slightly more abundant in the New Mexico samples. The small square arrowed in Fig. 1 illustrates the average size of crushed specimen chips examined in the transmission electron microscope. This size was well below the average grain size (0.45 cm in the New Mexico sample and 0.29 cm in the South Africa sample). As a result of this large grain size and the additional observation that fracture occurred in many thin sections at the grain boundaries, it was considered unlikely that grain boundaries or growth twin boundaries would be observed, and indeed we saw no grain boundaries in any samples in the electron microscope.

Fig. 2 shows several twins which, as a result of their irregularities and small size, are considered to be mechanical (deformation) twins and not growth twins, as observed in Fig. 1. Fig. 2a shows ledges in the boundary plane which are probably twinning dislocations. Fig. 2c shows numerous parallel twins, some having widths of the order of small annealing twins in FCC metals and alloys [13], and some having narrow widths, and resembling deformation twins and twin-faults in FCC metals and alloys [13–15].

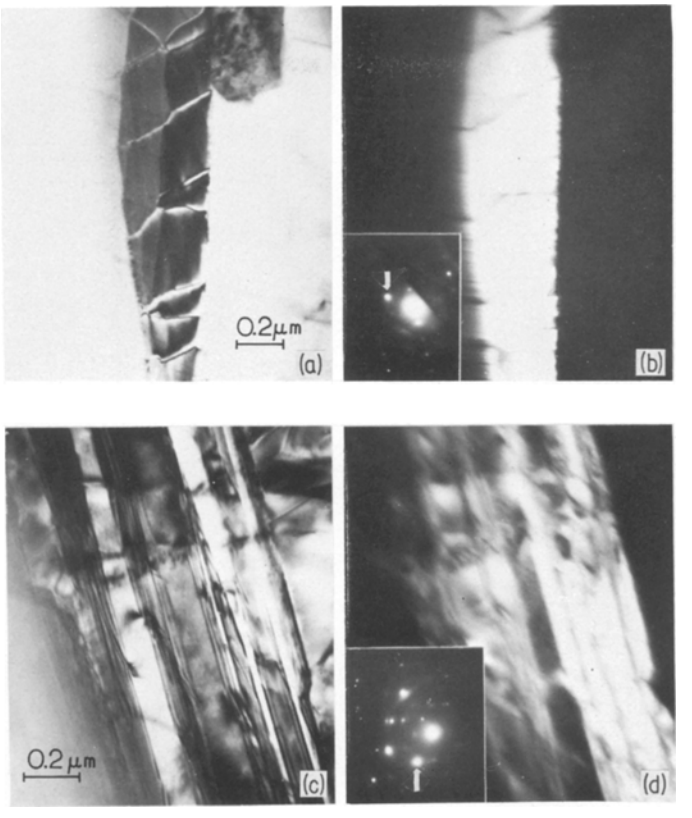

Figure 2 Mechanical twins in chalcopyrite. (a) Bright-field image of thin twin containing twinning dislocations appearing as ledges in the boundary plane. (b) Dark-field image of twin in (a) using $\bar{2}\,2\,0$ reflection arrowed in superimposed selected-area electron diffraction pattern. Surface orientation near (1 1 0). (c) Numerous, overlapping mechanical twins observed in bright-field. (d) Dark-field image of (c) using the arrowed $\bar{1}\,3\,2$ reflection in the superimposed selected-area electron diffraction pattern. The selected-area electron diffraction patterns have been rotated into approximate coincidence with the corresponding images. Note small streaks and extra reflections approximately normal to the trace direction (line of intersection of the $\{1\,1\,2\}$ twin plane with the specimen surface).

Fig. 3 illustrates several examples of single stacking faults and closely overlapping stacking faults giving rise in some areas to very thin twins; a prominent occurrence in deformed FCC alloys of low stacking-fault energy [13–16]. In Fig. 3a the nature of the outer fringe varies from bright (B) to dark (D) along various fault portions. As the contrast is governed by a strong 2-beam condition ($\mathbf{g} = [\bar{2}0\bar{4}]$), and considerable absorption occurs, the phase angle ($\alpha = 2\pi\mathbf{g}\cdot\mathbf{R}$) is observed to be $+2\pi/3$ at segments where the outer fringe is bright (B) and $-2\pi/3$ at segments where the outer fringe is dark (D) [17]. Thus both intrinsic and extrinsic faults are present. The extrinsic faults, however, appear to result where intrinsic faults overlap on adjacent {112} planes. This feature has been observed in deformed FCC alloys [13–16]. In Fig. 3b, several widely spaced intrinsic stacking faults are shown. The small fault at A shows clear 2-beam contrast conditions where the front partial is visible and the trailing partial bounding the stacking-fault region is invisible. Although the faulted plane is $(11\bar{2})$, it coincides with the $(11\bar{1})$ plane in the disordered lattice of sphalerite. Clearly, therefore, the trailing partial at A in Fig. 3b has a Burgers vector referred to the sphalerite lattice of $1/6[21\bar{1}]$, so that $\mathbf{g}\cdot\mathbf{b} = 0$ for the $[\bar{2}0\bar{4}]$ diffracting vector. The front partial, is then $1/6[1\bar{1}\bar{2}]$ ($\mathbf{g}\cdot\mathbf{b} = -1$]; indicating a dissociation of a total dislocation having a Burgers vector of $1/2[10\bar{1}]$ referred to the sphalerite lattice.

Fig. 4 shows dislocation arrays and nodes at intersecting dislocation lines. The dislocations in the network of Fig. 4b appear in most cases to be separated by a narrow region of stacking fault, i.e.

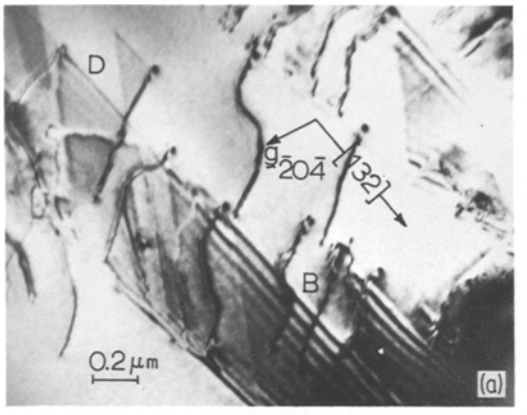

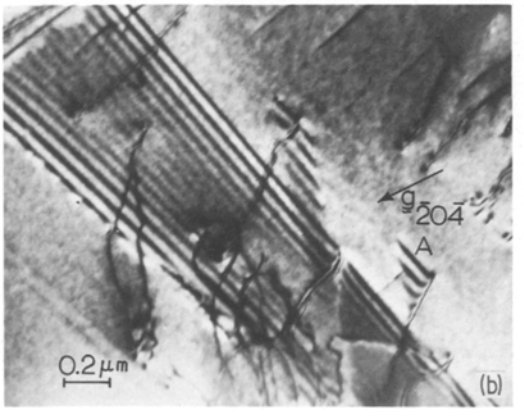

Figure 3 Bright-field electron micrographs of stacking faults in chalcopyrite ($CuFeS_2$). (a) Single and overlapping stacking faults. Variations in outer fringe nature at (B) and (D) give rise to changes in the sign of the phase angle and are indicative of both intrinsic and extrinsic stacking faults. (b) Large single stacking fault and smaller short ribbons of stacking fault bounded by visible and invisible partial dislocations (A). The operating reflection is shown in (a) and (b). The surface orientation in (a) and (b) is close to (2 0 $\bar{1}$).

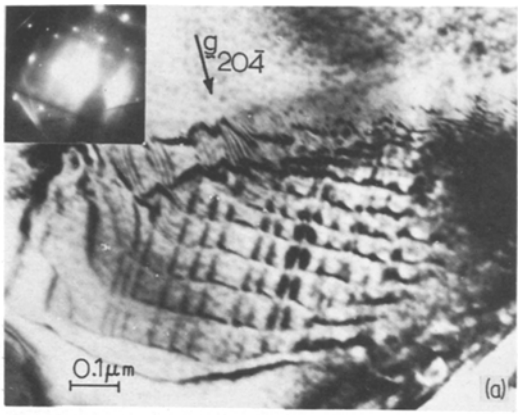

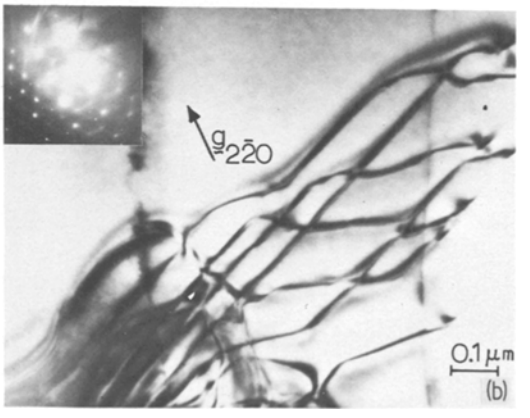

Figure 4 Dislocation substructure in natural $CuFeS_2$: (a) regular dislocation array, (b) irregular dislocation array and dislocation nodes at intersecting dislocation lines.

they appear in contrast as partial dislocations. While the diffraction conditions indicate a strong 2-beam situation, at least one additional beam may be contributing to the image contrast, giving rise to the weaker double dislocation image apparent in some portions of the electron micrograph. Complex dislocation images and double image contrast at dislocations in chalcopyrite were common in situations which were not strictly 2-beams or strong beam diffraction conditions. Several dislocation image irregularities occur at the leading partial at A in Fig. 3b and several dislocation images in Fig. 3a, and similar image perculiarities have been noticed at the dislocations observed in the $ZnSiP_2$ structure by Pasemann *et al.* [6], and in other mineral structures [12]. One reason for this apparent deviation from 2-beam diffraction conditions might be the irregular surface features created in preparing the electron-transparent sections by crushing larger specimens.

4. Discussions

The analysis of selected-area electron diffraction patterns in the present work was undertaken by using lattice parameters $a = 5.28$ Å and $c = 10.41$ Å [18]. These were observed to fit exactly most reflections observed, the only difficulty being the distinction between $\{2\,2\,0\}$ and $\{0\,2\,4\}$ reflections for which the calculated interplanar spacings correspond to 1.865 and 1.854 Å respectively. While Pauling and Brockway [19] determined the chalcopyrite ($CuFeS_2$) structure to have the space group $D_{2d}^{12} = 1\,\bar{4}\,2d$ with $a = 5.24$ Å, and $c = 10.30$ Å; the c/a ratio is essentially the same ($c/a = 1.966$) as that for the lattice parameters actually used here ($c/a = 1.972$). This ratio is sufficiently close to 2 that, as indicated previously, the chal-

copyrite structure approximates the sphalerite lattice. This would give rise to the types of crystal defects which normally occur in the sphalerite lattice, and would not include antiphase boundaries and superlattice dislocations. Indeed, unlike the previous TEM studies of the $ZnSiP_2$ chalcopyrite structure [6], no evidence was found in the present investigation for superlattice dislocations of the type 1/4 ⟨2 0 1⟩ in the $CuFeS_2$ chalcopyrite structure. Superdislocations having Burgers vectors of the type 1/4 ⟨2 0 1⟩ in the chalcopyrite structure correspond to a pair of perfect dislocations of the type 1/2 ⟨1 1 0⟩ in the disordered sphalerite lattice [6]. Since the $ZnSiP_2$ chalcopyrite structure has $c/a = 1.933$ ($a = 5.41$ Å, $c = 10.45$ Å) [3], it may be that the larger deviation from 2 for the $ZnSiP_2$ structure as compared with the $CuFeS_2$ structure can account for the absence of superlattice dislocations in the $CuFeS_2$. The chalcopyrite structure would therefore appear to be an interesting system in which to study the occurence of superdislocations, and it would be of interest to systematically observe the defect microstructures in $ZnSnP_2$ ($c/a = 2.000$), $ZnGeP_2$ ($c/a = 1.961$), and $CdGeP_2$ ($c/a = 1.876$) to see if the occurrence and structure of superlattice dislocations is dependent upon the c/a ratio. The occurrence of superdislocations in chalcopyrite structures might be expected to decline with an increase in temperature and eventually to disappear, since it is well known that the c/a ratio increases with temperature for most chalcopyrite structures. High temperature X-ray powder studies of $ZnGeP_2$ for example have shown that the c/a ratio increases from 1.961 to 2.000 between 20 and 950° C. Differences in the occurrence of superdislocations in the chalcopyrite structure might partially account for differences in the electronic (semiconducting) behavior of $A^{II}B^{IV}C_2^V$ compounds in particular [1, 4]. In addition, the differences to be expected in the defect structures in chalcopyrite crystals would also account in part for differences in physical and mechanical behavior [1, 3, 4].

One of the interesting observations in the present investigation has been the occurrence of both intrinsic and extrinsic stacking faults and deformation twins or twin faults. The occurrence of extended partial dislocations and wide ribbons of stacking-fault region is indicative of a fairly low stacking-fault free energy, perhaps in the range of 20 to 40 mJ m^{-2} (ergs cm^{-2}) when compared with FCC alloys [18]. These observations would tend to suggest that highly deformed chalcopyrite would contain large numbers of deformation microtwins and twin faults, and such faults might even characterize the growth of $CuFeS_2$ single crystals. If deformation twinning represents an important response to stress in the $CuFeS_2$ structure, then this may be an important factor in the leaching of chalcopyrite concentrates ground to very small size ranges [7, 9].

5. Summary and conclusions

This investigation represents the first complete study of defect structure in natural chalcopyrite ($CuFeS_2$). Dislocation loops, dislocation tangles and substructure (including networks of dislocations) stacking faults (both intrinsic and extrinsic), and mechanical twins and twin faults were observed. The examination of several natural sections revealed large grain sizes with frequent twins, some commensurate with the average grain size. It is concluded that the absence of superdislocations of the type 1/4 ⟨2 0 1⟩ in the natural chalcopyrite examined is the result of the $CuFeS_2$ structure accommodating more easily to the sphalerite lattice. The observations suggest a relatively low stacking-fault free energy in the range 20 to 40 ergs cm^{-2}, and a proficiency to twin readily at large deformation. It is suggested that the defect microstructure of $CuFeS_2$ can account in part for its particular electrical and mechanical properties, and that alterations in the microstructure of chalcopyrite crystal lattices might account in large part for the difference in such properties as they exhibit.

Acknowledgments

This work was supported in part by a National Science Foundation Grant (RANN) (AER-7603758) through the John D. Sullivan Center for *In-Situ* Mining Research. One of us (S.L.L.) wishes to acknowledge support through a Battelle-Sullivan Fellowship. The help of Dr J. B. Hiskey in acquiring the natural chalcopyrite samples for this study and his continued interest are gratefully acknowledged, as well as the assistance of Dr C. H. Ma in obtaining satisfactory X-ray data. The authors are also grateful for the extensive comments and corrections made by the referee on the original manuscript.

References

1. A. S. BORSHCHEVSKII, N. A. GORYUNOVA, F. KESAMANCY, and D. N. NASLEDOV, *Phys. Stat. Sol.* **21** (1967) 9.

2. B. RAY, *J. Mater. Sci.* **2** (1967) 284.
3. S. A. MUGHAL, A. J. PAYNE, and B. RAY, *J. Mater. Sci.*, **4** (1969) 895.
4. "Ternary Chalcopyrite Semiconductors", edited by J. L. Shay and J. H. Wernick, Vol. 7 of International Series on Surface Science of the Solid State (Pergamon Press, New York, 1975).
5. M. PASEMANN and P. KLIMANEK, *Kristall und Technik* **8** (1973) 1141.
6. M. PASEMANN, P. KLIMANEK, and H. OETTEL, *Phys. Stat. Sol. (a)* **22** (1974) K1.
7. J. K. GERLACH, E. D. GOCK and S. K. GHOSH, "International Symposium on Hydrometallurgy", edited by D. J. I. Evans and R. S. Shoemaker (American Inst. of Mining, Metallurgical and Petroleum Engrs., New York, 1972) p. 403.
8. F. P. HAUER and M. M. WONG, *J. Metals* (Feb. 1971) 25.
9. J. GERLACH, F. PAWLEK, R. RÖDEL, G. SCHÄDE, and H. P. WEDIGGE, *Erzmetall* **25** (1972) 448.
10. Y. MONFORT, J. VIZOT, and A. DESCHANVRES, *Phys. Stat. Sol. (a)* **29** (1975) 551.
11. C. S. BARRETT and T. B. MASSALSKI, "Structure of Metals", (McGraw-Hill, New York, 1966).
12. "Electron microscopy in mineralogy", edited by H. -R. Wenk, P. E. Champness, J. M. Christy, J. M. Cowley, A. H. Heuer, G. Thomas, and N. J. Tighe (Springer Verlag, New York, 1976).
13. L. E. MURR, "Electron Optical Applications in Materials Science" (McGraw-Hill, New York, 1970).
14. L. E. MURR and F. I. GRACE, *Experimental Mechs.* **5** (1969) 145.
15. L. E. MURR and K. P. STAUDHAMMER, *Mater. Sci. Engr.* **20** (1975) 35.
16. L. E. MURR, *Thin Solid Films* **4** (1969) 389.
17. H. HASHIMOTO, A. HOWIE, and M. J. WHELAN, *Proc. Roy. Soc.* **A269** (1962) 80.
18. A. K. HEAD, P. HUMBLE, L. M. CLAREBROUGH, A. J. MORTON, and C. T. FORWOOD, "Computed Electron Micrographs and Defect Identification", (North-Holland, London, 1973).
19. L. E. MURR, "Interfacial Phenomena in Metals and Alloys", (Addison-Wesley, Reading, Mass., 1975).

Received 25 October and accepted 16 December 1976.